On chemical and diffusional interactions between PCBN and superalloy Inconel 718

Imitational experiments

Bushlya, V.; Bjerke, A.; Turkevich, V. Z.; Lenrick, F.; Petrusha, I. A.; Cherednichenko, K. A.; Ståhl, J. E.

Published in:
Journal of the European Ceramic Society

DOI:
10.1016/j.jeurceramsoc.2019.03.002

2019

Document Version:
Early version, also known as pre-print

On chemical and diffusional interactions between PCBN and superalloy Inconel 718: imitational experiments

V. Bushlya,[1]* A. Bjerke,[1] V.Z. Turkevich,[1,2] F. Lenrick,[1] I.A. Petrusha,[2] K.A. Cherednichenko,[3] J.-E. Ståhl,[1]

[1]Division of Production and Materials Engineering, Lund University, Ole Römers väg 1, Lund, Sweden

[2]Institute for Superhard Materials, NAS of Ukraine, Avtozavodska 2, Kiev, Ukraine

[3]LSPM–CNRS, Université Paris Nord, 93430 Villetaneuse, France

volodymyr.bushlya@iprod.lth.se

Abstract

During a metal cutting process, chemical wear can become the dominant mechanism of tool degradation under the high temperatures and contact pressures that arise between the tool and the metal workpiece. This study focuses on the chemical and diffusional interactions between superalloy Inconel 718 and cubic boron nitride (cBN) tool material with and without TiC binder. It covers thermodynamic modeling and experimental tests in the pressure range of 0.1 Pa to 2.5 GPa at temperatures up to 1600 °C. The methods used include diffusion couples under both vacuum and high pressure, transmission electron microscopy (TEM) analysis and *in-situ* synchrotron observations. It is shown that cBN is prone to diffusional dissolution in the metal and to reactions with niobium, molybdenum, and chromium from Inconel 718. Adding TiC binder changes the overall degradation process because it is less susceptible to these interaction mechanisms.

Keywords: PCBN; Inconel 718; diffusional wear; chemical wear; diffusion couple

1. Introduction

Polycrystalline cubic boron nitride (PCBN) tools are widely used in machining hardened steels and superalloys due to their high hardness, wear resistance, and thermal conductivity. These beneficial mechanical and thermal properties are slightly lower than those of polycrystalline diamond. However, PCBN is substantially more chemically inert than polycrystalline diamond. At high cutting speeds, the advantage of the high hardness and abrasion resistance loses its significance because chemical and diffusional mechanisms are activated as the cutting process temperatures increase [1].

While there is evidence of chemical and diffusional mechanisms with cemented carbide tooling [2–4], less is known about PCBN tooling. A diffusion couple study [5] of cubic boron nitride and elemental iron did not register a chemical interaction. Another diffusion couple study of iron and PCBN with TiC binder carried out under vacuum showed that chemical interaction occurs at temperatures above 1300 °C [6]. The authors of that study demonstrate that the interaction is related to the binder and not to cBN. The mechanism was believed to be formation of cementite due to dissolution of carbon from the TiC binder. A diffusion couple study of PCBN with austempered ductile iron also indicated reactions between iron and silicon from the workpiece with the TiC binder phase and not with the cBN phase [7].

Oxidation of PCBN, another type of chemical interaction, has also been investigated. The presence of boron oxide among the wear products on a PCBN tool has been experimentally verified [8]. Similarly, oxidation wear of PCBN has been found in machining hardened tool steel, activated only under accelerated process conditions [9].

More complications are introduced when machining alloyed materials containing Cr, Ni, Mo, Nb, etc., such as hardened tool steels or superalloys as there are indications of the formation of metal borides and their subsequent eutectic melting [10]. The chemical reactivity of cBN and elemental nickel when annealing compacted powders in vacuum at 1300 °C results in the formation of nickel borides [11].

There has, however, been no extensive study of the reactivity between PCBN and highly alloyed workpiece materials. This study thus focuses on chemical and diffusional interaction of PCBN in machining superalloys.

When machining superalloys, temperatures as high as 1250 °C are reached in the cutting zone [12]. High contact pressures also develop there, with estimated average pressures of up to 2.5 GPa [13]. Therefore, in this study, thermodynamic calculations were experimentally compared to three *imitational situations* to investigate the effect of temperature and pressure on chemical and diffusional interactions of PCBN with superalloy Inconel 718 (also known as Alloy 718). The three *imitational situations* were:

1. Low vacuum (0.1 Pa) annealing of powdered PCBN and Inconel 718 mixture
2. High pressure (2.5 GPa) annealing of powdered PCBN and Inconel 718 mixture
3. High pressure (2.5 GPa) annealing of bulk PCBN and Inconel 718 (diffusion couple)

These *imitational situations* were designed to reproduce different aspects of metal cutting relevant to chemical and diffusional wear. Specifically, the influence of pressure and diffusion length were set as key variables. Additionally, the influence of PCBN composition on the interaction was investigated. It is known that high-cBN tools have a higher wear rate in continuous machining than low-cBN materials with ceramic binders [14]. Therefore, this study also aims to investigate the mechanisms responsible for the discrepancy in wear between high- and low-cBN tool materials. For each of the *imitational situations* two cases were examined: high-cBN material (case H) and low-cBN material with TiC binder (case L).

The powder samples treated in low vacuum (*imitational situation* 1) were annealed at temperatures ranging from 900 °C to 1250 °C. These samples were later analyzed using laboratory source X-ray diffraction (XRD). The powder samples annealed under high pressure (*imitational situation* 2) were analyzed *in-situ* from 20 °C to 1600 °C using synchrotron source energy dispersive X-ray diffraction (EDXRD). A constant pressure of 2.5 GPa was applied to these samples. The bulk diffusion couple samples annealed at high pressure (*imitational situation* 3) consisted of round tool inserts placed in Inconel 718 capsules and heated to 1300 °C at a constant pressure of 2.5 GPa. These samples were later analyzed using TEM.

2. Materials and Methods

As can be seen in Fig. 1a, the microstructure of commercial aged Inconel 718 includes six phases: Ni-γ solid solution with face-centered cubic (FCC) crystal structure; γ' FCC $Ni_3(Ti,Al)$ precipitates; γ'' precipitates of body-centered tetragonal (BCT) structured Ni_3Nb; δ orthorhombic Ni_3Nb; and the carbides NbC and TiC. The δ Ni_3Nb phase forms plate-like precipitates at the grain boundaries (Fig. 1c). Aged Inconel 718 material in a machining operation initially includes all the phases listed above; however in the machining process the precipitates (γ', γ'', δ) are dissolved into the Ni-γ phase [15–16], creating a supersaturated solution in the near surface region. This means that in high speed machining, the tool material interacts with solutionized Inconel 718 instead of multi-phase aged material. To insure that the Inconel 718 was also solutionized in the three *imitational situations* tested, a high pressure high temperature (HPHT) experiment on commercial aged Inconel 718 was conducted. A solid cylindrical block of aged Inconel 718 was subjected to flash HPHT treatment (2.5 GPa and 1300 °C) involving rapid heating (250 °C/s) and immediate quenching. XRD analyses prior to and after the HPHT treatment are shown in Fig. 1a and 1b. The data show dissolution of the precipitates (γ', γ'', δ) and carbides into the Ni-γ solid solution during the short treatment time. Such rapid dissolution indicates that the material phase composition present at the beginning of the *imitational situations* is the same as in high speed machining.

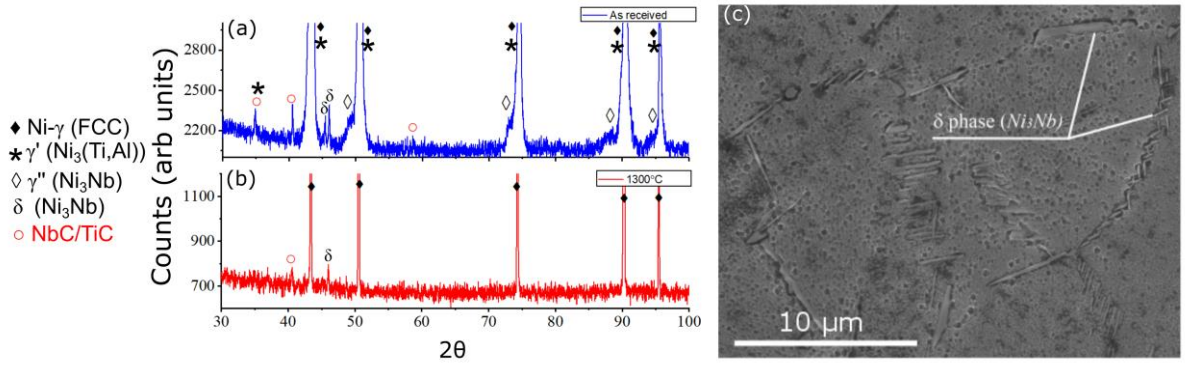

Fig. 1. *Microstructure of Inconel 718: (a) XRD analysis of as received aged Inconel 718, (b) XRD analysis of the HPHT treated Inconel 718 and (c) SEM image of as received Inconel 718.*

Situation 1 and 2 use powdered materials to yield large quantities of reaction products and so facilitate their detection. The difference between *situation* 1 and 2 is the pressure used. *Situation* 2 employs high pressure to imitate high speed machining, while *situation* 1 under low vacuum and reflects a conventional high-throughput setup. *Situation* 3 uses bulk materials in a diffusion couple arrangement. This *situation* imitates both diffusional dissolution (mass transport) and chemical reactivity. The downside is that smaller amount of reaction products are formed, which means it is more difficult to detect them.

For the *situations* involving powder material (1 and 2), cBN powder was synthesized at the Institute for Superhard Materials from hexagonal BN (hBN) in a catalyst-solvent system of magnesium and its compounds. Powdered TiC was supplied by H.C. Starck, while LPW Technology LTD supplied gas atomized powder of Inconel 718 in solutionized state with the composition shown in Table 1. For *situation* 3, two grades of PCBN tool material were selected to represent case H and case L. Case H is a binderless cBN grade (BCBN) which has 5-7 µm cBN grains and 3% stress-inducing inclusions of β-Si3N4 (see Fig. 2a and 2b). Case L is a commercial low-cBN content grade by Seco Tools AB (L-CBN) with a TiC-based binder and other secondary phases (see Fig. 2c and 2d), constituting approximately 50% by volume. Commercial aged Inconel 718 was supplied by Siemens Industrial Turbomachinery AB (see Table 1).

Before vacuum annealing in *situation* 1, the powders were dry mixed in ratios representing the tools in case H and case L (see Table 2) and cold pressed in a cemented carbide die at 2.5 GPa. The compacted pellets were annealed in a low vacuum furnace (see Table 2), and then sectioned, polished and analyzed using XRD and SEM/XEDS. *Situation* 2 tests were conducted at the PSICHÉ beamline, SOLEIL synchrotron in France, using the Paris−Edinburgh press and 10 mm assembly equipped with graphite resistive heater [17]. The mixed powders for both cases were placed into hBN capsule and, thus were shielded from graphite furnace. Energy dispersive X-ray diffraction (EDXRD) patterns were recorded during heating at intervals of 25 °C. The pressure values at room temperature were estimated using hBN equation of states [18], whereas temperature was controlled with help of the corresponding power (W)-temperature (°C) calibration curve [17]. EDXRD patterns were collected in white beam mode (25-80 keV) using Canberra solid state Ge-detector with angle fixed to 8.021°.

The heating rate was set to 20 °C/min, EDXRD acquisition time was 1 min. The overall conditions are listed in Table 2.

	Ni	Cr	Fe	Mo	Nb	Ti	Al	Co	Cu	Mn	Si	C	P	S
Bulk	bal.	18.2	17.8	2.92	5.04	1.01	0.32	0.17	0.04	0.06	0.07	0.03	0.008	0.001
Powder	bal.	19.0	18.0	3.0	5.0	1.0	0.5	–	–	–	–	0.04	–	–

Table 1. *Chemical composition of Inconel 718 by wt. %.*

Imitational situation	**Pressure**	**Temperature** range [°C]	**Case**	Powder mixture ratio [wt.%], or bulk sample	**A718** powder particle size [μm]	**cBN** powder particle size [μm]	**TiC** powder particle size [μm]	**Duration** [min]
1	< 10^{-1} Pa	900-1250	H	cBN: 29.8 A 718: 70.2 TiC: 0.0	15–45	14–20	-	120
			L	cBN: 14.1 A 718: 19.9 TiC: 66.0	15–45	14–20	1.5–2	120
2	2.5 GPa	25-1600	H	cBN: 29.8 A 718: 70.2 TiC: 0.0	15–45	14–20	-	100
			L	cBN: 14.1 A 718: 19.9 TiC: 66.0	15–45	14–20	1.5–2	100
3	2.5 GPa	1300	H	6.35 mm ø BCBN insert	Bulk	Bulk	-	5
			L	6.35 mm ø L-CBN insert	Bulk	Bulk	Bulk	5

Table 2. *Conditions for the treatments in the three imitational situations.*

For *situation* 3, the diffusion couples were subjected to high pressure and heated using an hBN-sleeved graphite heater in the conditions shown in Table 2. A toroid type high pressure apparatus [19] HPAT-30 was used for the treatment. Once the temperature and pressure had been reduced, the samples were cut in the axial direction, polished and analyzed using SEM, TEM, and XEDS.

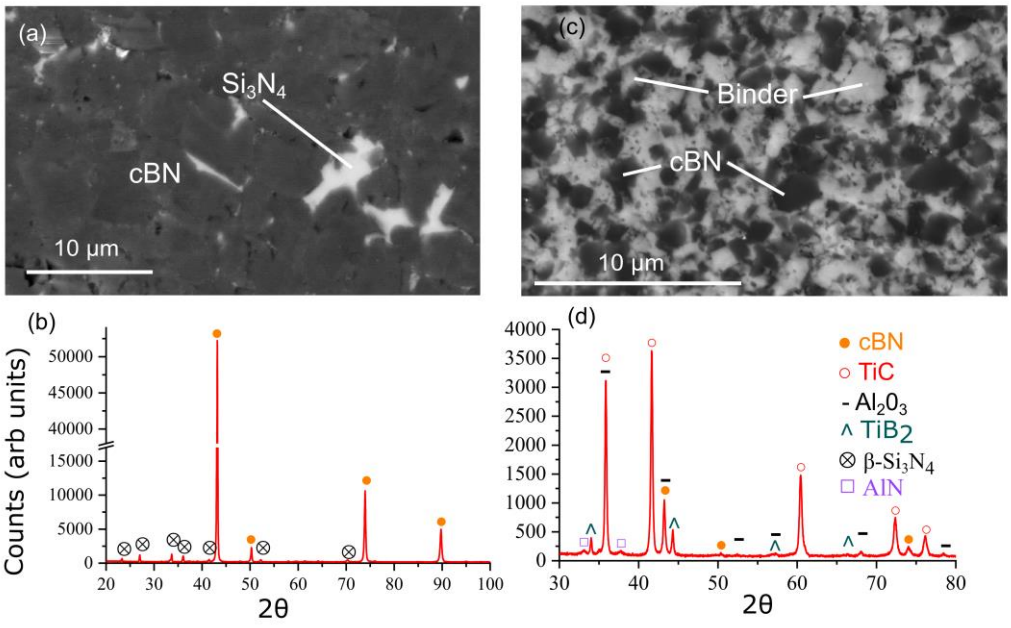

Fig. 2. *SEM and XRD showing the microstructure of the tool materials used in imitational situation 3: (a–b) case H, binderless cBN; and (c–d) case L, PCBN with TiC binder.*

The computer coupling of phase diagrams and thermochemistry (CALPHAD) method using Thermo-Calc [20] succeeds in evaluating the phase stability of Inconel 718 [21]. Thermo-Calc has also been successful in simulating diffusion and chemical interaction between a workpiece and cemented carbide tooling [2–3]. Thermo-Calc calculations of Inconel 718 at high pressure and high temperature have not been assessed in literature, and neither has the interaction between Inconel 718 and tool materials. Thermodynamic calculations of the interaction between the tool materials (case H and case L) and Inconel 718 were performed at pressures ranging from 0.1MPa to 2.5GPa for temperatures between 400 and 1700 °C.

3. Results and Discussion

3.0 Thermodynamic modeling

Thermodynamic modeling of the chemical interaction between the elements of case H and case L with Inconel 718 at 0.1 MPa was performed using Thermo-Calc. The TCNI8 database, which describes the properties of nickel superalloys and nickel compounds, was used. The results of the calculation are shown in Fig. 3a and 3c. Among the products at atmospheric pressure are borides and nitrides of molybdenum, chromium, iron, niobium, nickel, aluminum, and titanium. Case L with TiC binder also results in the formation of carbides of titanium, niobium, and chromium.

The influence of pressure on the expressions for the temperature dependence of the Gibbs energy can be added to the Thermo-Calc modeling by adding the change in Gibbs energy due to an increase in pressure to every phase. The values of the molar volumes of phases are taken from Landolt–Börnstein [22] and the Thermo-Calc TCNI8 databases. The bulk moduli and the coefficients of thermal expansion of all competing phases make a negligible difference to the results of the change in Gibbs energy between phases present. Thus, the bulk moduli and the coefficients of thermal expansion for competing phases were assumed to be equal. Fig. 3b and 3d show the modeling results at 2.5 GPa.

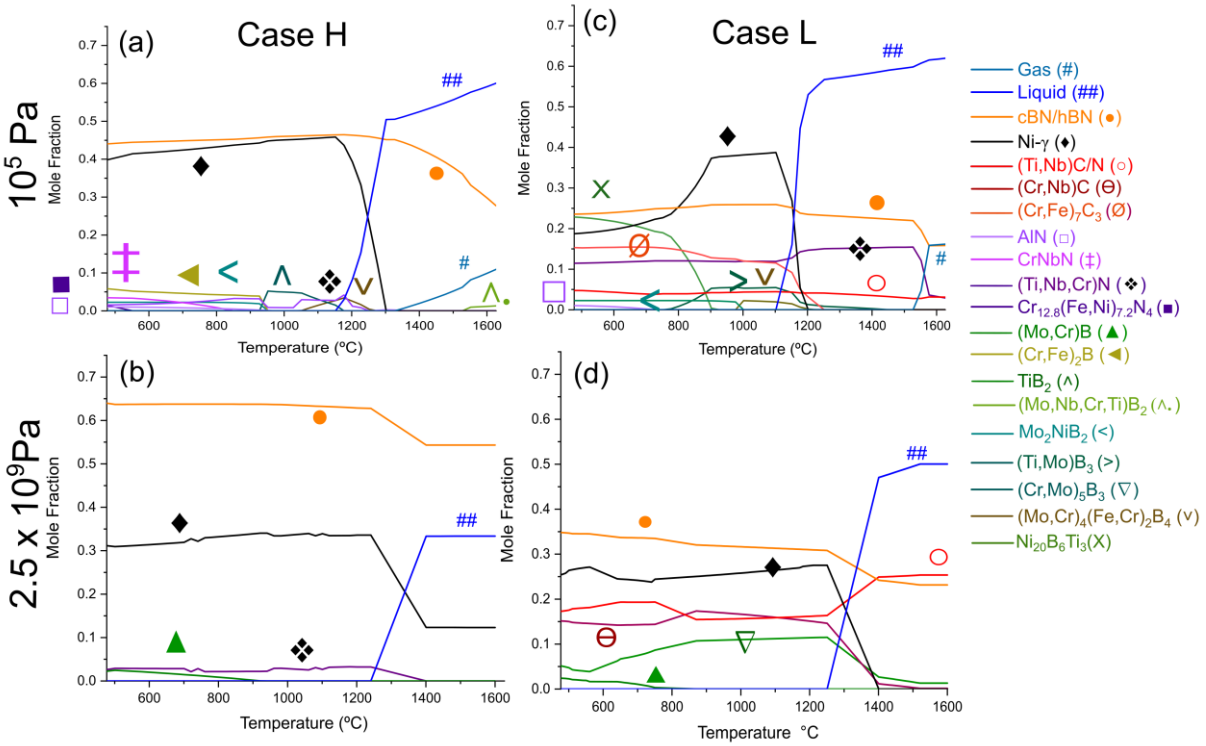

Fig. 3. *Results from thermodynamic calculations for case H (a-b) and case L (c-d).*

Applying pressure of 2.5 GPa significantly reduces the number of reaction products, as only phases with low specific volume remain stable at high pressures (Fig. 3b and 3d). Different configurations of (Mo,Cr)B, (Ti,Nb,Cr)N are stable in case H, while (Ti,Nb)C, (Cr,Nb)C and $(Cr,Mo)_5B_3$ are stable in case L due to the presence of the TiC binder. The temperature of initial melting increases by over 100 °C under high pressure.

3.1 *Imitational Situation* 1 – Vacuum annealing of powdered cBN and Inconel 718

The results from the XRD and SEM analysis in *imitational situation* 1 (Fig. 4) show the formation of reaction products. These new phases are identified by combining data from both XRD and XEDS. Chromium mono- and diboride and nickel boride are identified by XRD phase analysis. In the case of chromium boride, it corresponds to space group Cmcm with lattice parameters a = 0.298 nm, b = 0.787 and c = 0.293 nm. But XEDS indicates that the phase is rich in Cr, Mo, Nb and B; thus (Cr,Mo,Nb)B is identified as the reaction phase. Similarly, $(Cr, Mo)B_2$ and $(Ni, Fe, Nb)_{23}B_6$ are confirmed. It is worth noting that formation of nickel borides has been reported for vacuum annealing [11]. The eutectic of Ni-γ and nickel boride is also seen in Fig. 4b.

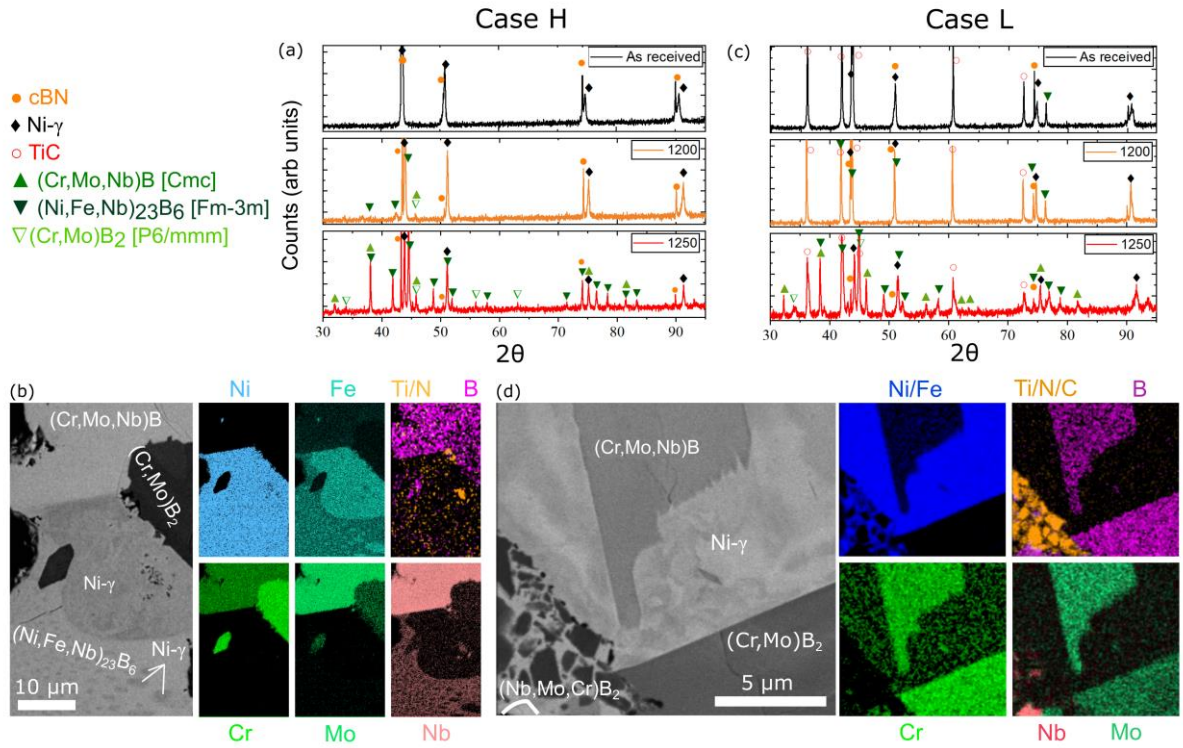

Fig. 4. *XRD and SEM/XEDS of the vacuum annealed powder samples in situation 1 at 1250 °C: case H in (a–b) and case L in (c–d).*

Attention should be drawn to the absence of nitrides among the interaction products. It is assumed that nitrogen does not participate in the reactions because it leaves the interaction system under vacuum as a gaseous phase due to cBN sublimation.

3.2 *Imitational Situation* 2 – High-pressure annealing of powdered cBN and Inconel 718

The EDXRD results of the synchrotron studies from *situation* 2 are shown in Fig. 5. In case H, the first observed reaction products were AlN and (Ti, Nb)N, detected above 350 °C. The AlN lines disappeared completely before the sample had reached 1000 °C, while (Ti, Nb)N was stable until 1400 °C and disappeared before 1500 °C. At around 1200 °C three metal borides, MoB, MoB_2 and CrB_2, were detected. These were joined by Cr_2B_3 at around 1500 °C. All four metal borides remain stable throughout the experiment and after quenching.

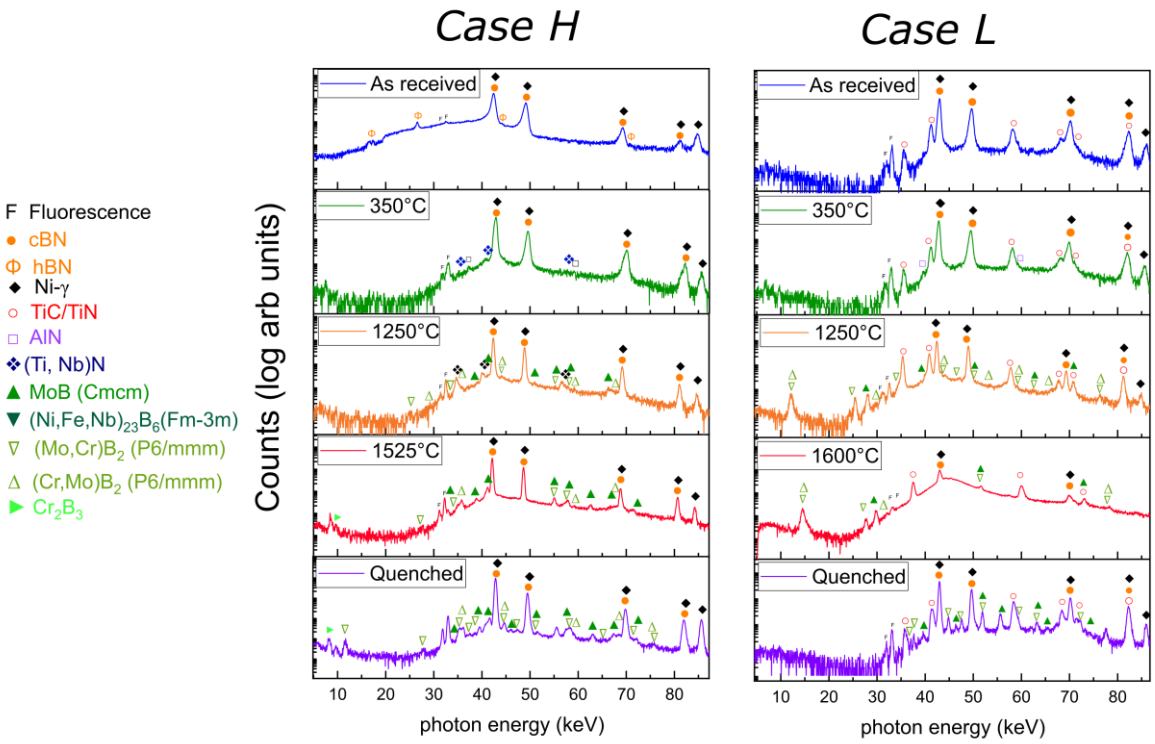

Fig. 5. In-situ EDXRD imitational situation 2.

In Fig. 6, *post-mortem* XEDS analysis of case H is shown for a sample quenched from 1250 °C and another sample quenched from 1600 °C. Quenching at 1250 °C leaves 10 µm large cBN grains surrounded by borides rich in Cr, Mo and Nb and nitrides rich in Ti and Nb. Quenching at 1600 °C leaves a network of Cr, Mo and Nb rich borides while no nitrides were found.

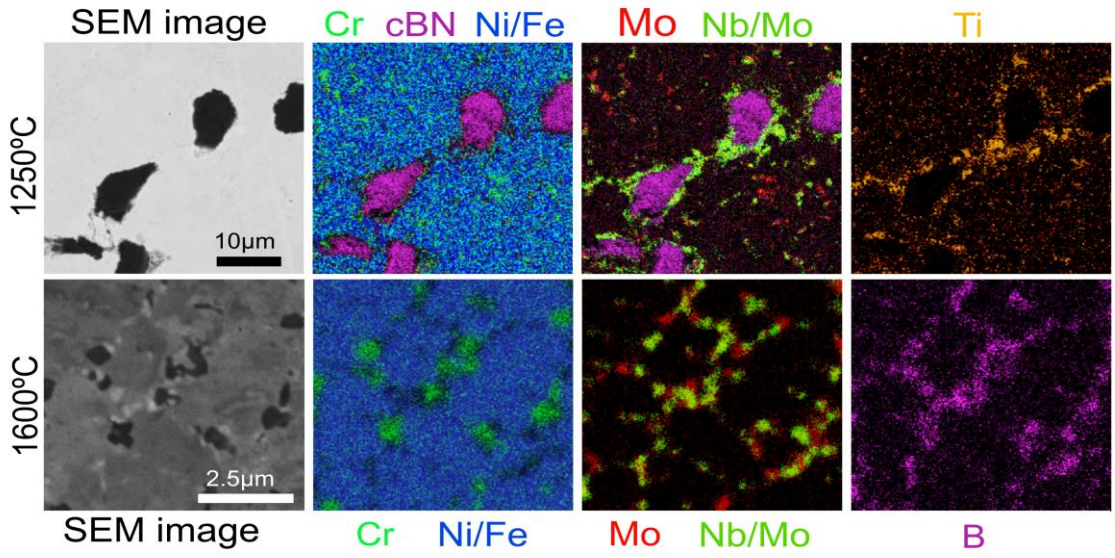

Fig. 6. Post-mortem SEM/XEDS of the quenched high pressure annealed powder samples in imitational situation 2.

AlN was also the first observed reaction product in case L. It appears at 350 °C and disappears before the sample reaches 1000 °C. No other nitrides were detected in this case,

although it is likely that the diffraction lines from many nitrides and carbonitrides overlap with the lines from TiC so that they are not conclusively identifiable. The metal borides MoB, MoB_2, and CrB_2 were detected at around 1200 °C, and Cr_2B_3 at around 1500 °C. Similarly to the thermodynamic calculations, the application of 2.5 GPa pressure shifts the melting point of Inconel 718 (Fig. 5, case L) compared to ambient conditions.

Residues of cBN phase in a sample quenched from 1250 °C were extracted by ultrasonically-assisted etching in an HF-based solution and compared to as received cBN powder. Fig. 7 shows the formation of pits due to diffusional dissolution of boron and nitrogen into Ni-γ solid solution during HPHT treatment. This confirms that diffusion is one of the active mechanisms in the wear of PCBN.

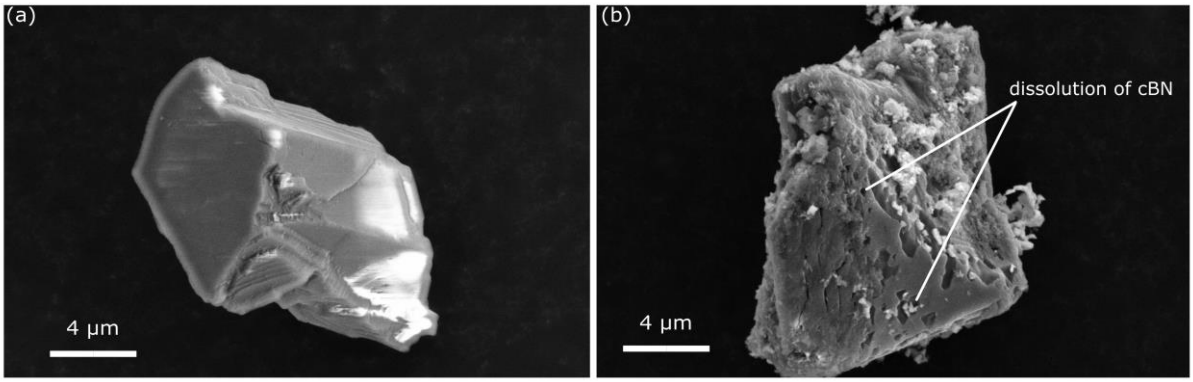

Fig. 7. *SEM images of cBN grains a) as received and b) after imitational situation 2 and etching. Dissolution pits can be seen in b) where partly dissolved cBN is visible.*

3.3 *Imitational Situation 3* – High-pressure annealing of bulk PCBN and Inconel 718

Fig. 8b shows a cross section of a high pressure annealed diffusion couple for case H. Both case H and L diffusion couples show an interaction layer at the interfaces with Inconel 718. Precipitation of new phases is observed primarily along the grain boundaries. Machining the Inconel 718 capsules resulted in sub-surface plastic deformation and reduced grain-size and a developed network of grain boundaries after annealing. Fig. 8a shows new precipitated phases in case H with an increased concentration of Nb, Mo, B, and partly N and Ti. A sharp increase in the concentration of C, Nb, Ti, Mo, B, and N was detected in case L, as seen in Fig. 8c. Reaction products were generally found up to 15 µm deep from the original interface.

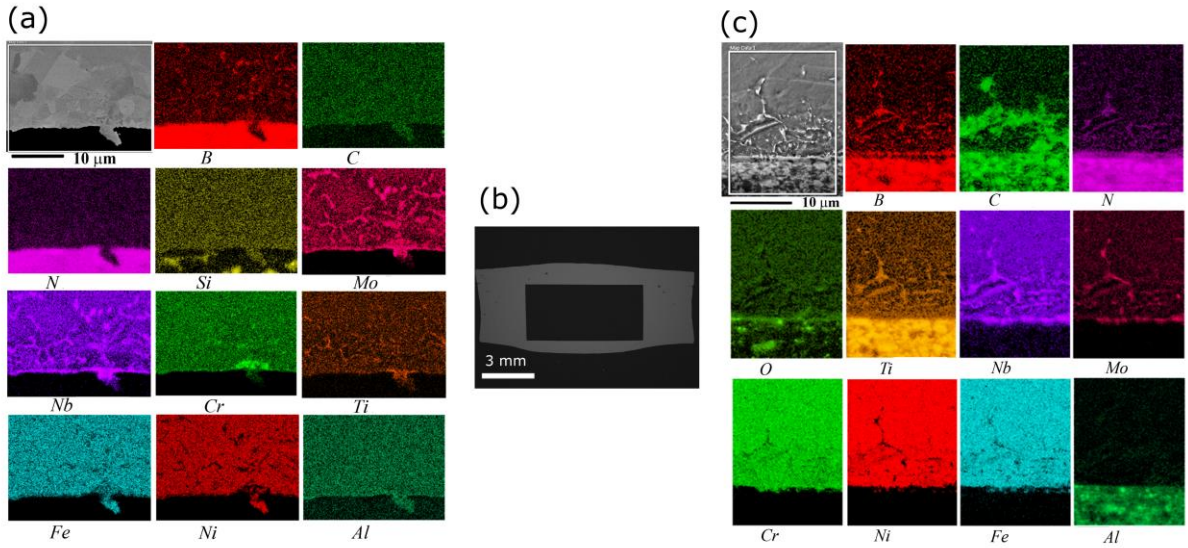

Fig. 8. *SEM/XEDS of diffusion couples in situation 3: (a) case H, (b) SEM overview of diffusion couple, and (c) case L.*

Fig. 9 shows that for case L diffusional dissolution of cBN grains takes place at the contact region between the PCBN insert and Inconel 718. Note that the same type of dissolution occurred in *imitational situation* 2 (Fig. 7). The locations occupied by cBN before high pressure annealing are replaced by a solutionized Ni-γ after treatment. The SEM image indicates the relative stability and invariable position of the TiC binder grains. At the same time, XEDS analysis shows an increase of the carbon content in the interaction layer due to diffusion. The source of this carbon, which diffuses into Ni-γ solid solution, is the TiC phase. An increase in the number of vacancies on the carbon sublattice of titanium carbide is possible without a collapse of the lattice at the elevated temperatures. Titanium carbide can reach a composition of $TiC_{0.7}$ at 1300 °C [23], which fully explains how TiC can remain stable while losing carbon to the counterface metal.

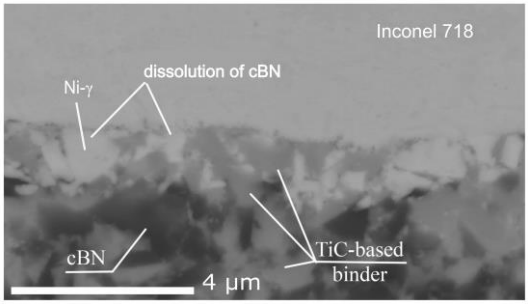

Fig. 9. *SEM image of dissolution of cBN in the Ni-γ solid solution in situation 3 case L.*

The original interface between PCBN and Inconel 718 can be identified by a trail of Al_2O_3 grains shown in the STEM HAADF (high-angle annular dark field) image and XEDS maps (Fig. 10). The oxygen trapped inside the diffusion couple capsule before annealing was limited, and after an initial oxidation of Al from Inconel 718, all oxygen would have remained in Al_2O_3 form during the high pressure annealing. The presence of this Al_2O_3 reference allows

quantitative measurement of diffusional loss (mass transport) of the cBN phase. No reaction products are found directly on the metal-cBN interface (Fig. 10), whereas Ni-γ is epitaxial to cBN.

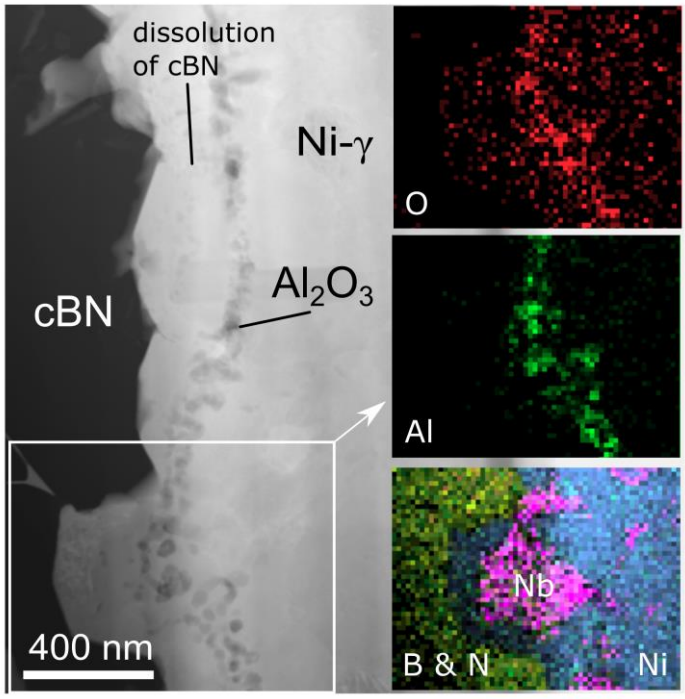

Fig. 10. STEM HAADF and XEDS of original interface and post-treatment interface, Imitational situation 3 case H.

Precipitates of (Nb, Ti)N were found inside the Inconel 718 grains and along the grain boundaries. These precipitates are shown in Fig. 11. The diffraction pattern is well-matched with epitaxial Ni-γ and (Nb, Ti)N, which causes extra, so-called double, diffraction spots. The precipitates are epitaxial with the Ni-γ phase (Fig 11a) as can be seen in the SAED in Fig. 11c. In case L, formation of carbonitrides was observed.

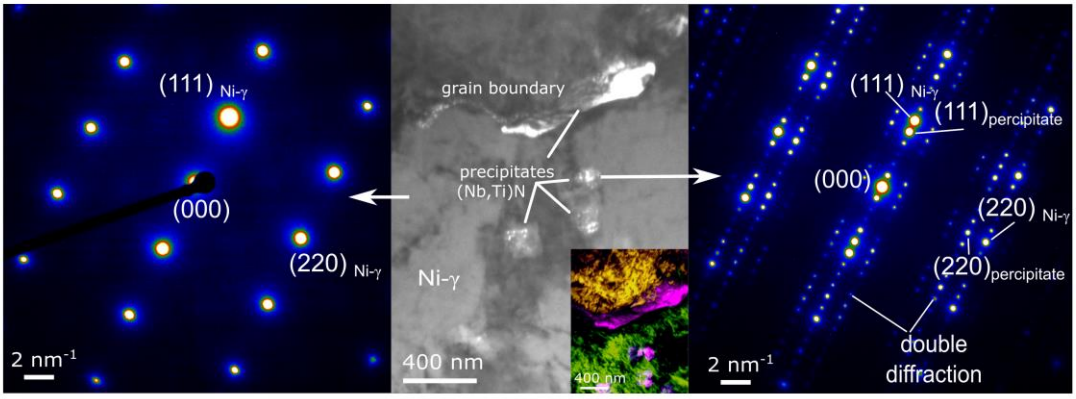

Fig. 11. Imitational situation 3 case H: (a) SAED image of Ni-γ area, (b) Overview TEM and false color DFTEM triplet and (c) SAED image of area with (Nb, Ti)N precipitates epitaxial with the Ni-γ solid solution.

Fig. 12 shows another reaction product, with approximate stoichiometry $(Cr, Nb)_3B_4$. The SAED pattern is shown in Fig. 12c and matches Nb_3B_4 well. These (Nb, Ti)N and $(Cr, Nb)_3B_4$

reaction products were found roughly 3 µm from the interface on the Inconel 718 side of the diffusion couple.

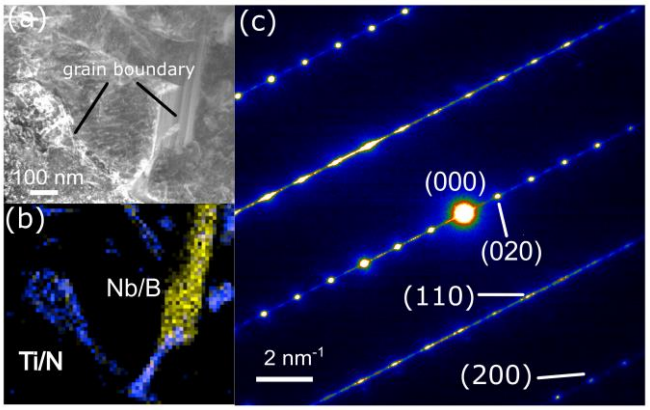

Fig. 12. *Imitational situation 3 case H: (a) STEM LAADF, (b) XEDS map of Ti/N and Nb/B, and (c) SAED image of* $(Cr, Nb)_3B_4$.

The thermodynamic modeling is in good agreement with both high pressure experimental series (case H and case L) where borides and nitrides of Nb, Cr, Mo, and Ti are formed. However, vacuum annealing, which results in nitrogen loss due to cBN sublimation, changes the interaction system. In this case, formation of nickel boride is observed. This $(Ni,Fe,Nb)_{23}B_6$ boride has a low temperature melting eutectic with Ni [24], as shown in Fig. 4a. This result shows that low-vacuum imitational situation is not representative of the machining conditions.

4. Conclusions

The paper addresses the mechanisms of diffusional and chemical interactions encountered under conditions similar to high speed machining of superalloy Inconel 718 with PCBN tools. The approach using *imitational situations* involves the use of thermodynamic modeling, low vacuum powder annealing, HPHT *in-situ* EDXRD of powders, and HPHT diffusion couples of both high-cBN and low-cBN tool materials.

The results of thermodynamic modeling and *imitational situations* 2 and 3 are in reasonable agreement. The annealing under low vacuum in *imitational situation* 1 leads to a loss of nitrogen and formation of nickel boride, which creates a low temperature eutectic with Ni-γ solid solution.

Under high pressure (2.5 GPa) and high temperature (up to 1600 °C), conditions that are often reached in machining, the mechanisms of interaction include the diffusion of boron and nitrogen from cBN into Inconel 718, formation of their solid solutions, saturation and precipitation of new phases. In this way, the diffusional mechanism is responsible for the loss of cBN, while formation of nitrides of Ti and Nb and borides of Cr, Mo, and Nb governs the chemical interaction.

Both experimental and theoretical results show that presence of titanium carbide binder in PCBN (case L) changes quantitative aspects of the interaction. Despite the diffusional loss of carbon, TiC remains more stable than cBN and acts as an inert obstacle to further diffusional loss of the cBN phase. The results obtained make it possible to explain the significantly lower wear rate of PCBN tools with low-cBN content and ceramic binders compared to grades with high-cBN.

Acknowledgments

This research was supported by the European Union's Horizon 2020 Research and Innovation Programme under the Flintstone2020 Project (grant agreement No. 689279). The acknowledgment also extends to the Sustainable Production Initiative - a cooperation between Lund University and Chalmers University of Technology. The authors are grateful to Dr. Y. Le Godec for assistance at beamline PSICHÉ, SOLEIL, and Prof. V.L. Solozhenko (LSPM-CNRS) for helpful discussions. The *in-situ* high-pressure experiments were carried during beamtime kindly provided by SOLEIL.

References

[1] Y. Huang, Y. K. Chou and S. Y. Liang, CBN tool wear in hard turning: A survey on research progresses, The International Journal of Advanced Manufacturing Technology 35 (5–6) (2007) 443–453.

[2] O. Hatt, H. Larsson, F. Giuliani, F., P. Crawforth, B. Wynne, M. Jackson, Predicting Chemical Wear in Machining Titanium Alloys Via a Novel Low Cost Diffusion Couple Method, Procedia CIRP 45 (2016) 219–222.

[3] S. Odelros, B. Kaplan, M. Kritikos, M. Johansson, S. Norgren, Experimental and theoretical study of the microscopic crater wear mechanism in titanium machining, Wear 376-377 (2017) 115-124.

[4] L. von Fieandt, R. M'Saoubi, M. Schwind, B. Kaplan, C. Århammar, B. Jansson, Chemical Interactions Between Cemented Carbide and Difficult-to-Machine Materials by Diffusion Couple Method and Simulations, Journal of Phase Equilibria and Diffusion 39 (4) (2018) 369–376.

[5] N. Narutaki N. and Y. Yamane, Tool wear and temperature of cBN tools in machining of hardened steels, Annals of CIRP 28 (1) (1979) 23–28.

[6] S. Gimenez, O. Van der Biest, J. Vleugels, The role of chemical wear in machining iron based materials by PCD and PCBN super-hard tool materials, Diamond and Related Materials 16 (2007) 435–445.

[7] K. Katuku, A. Koursaris, I. Sigalas, Structural features of the austempered ductile iron-PcBN cutting tool interaction interface as captured through static diffusion couple experiments, Solid State Ionics 224 (2012) 41–50.

[8] K. Katuku, A. Koursaris, I. Sigalas, Wear mechanisms of PCBN cutting tools when dry turning ASTM Grade 2 austempered ductile iron under finishing conditions, Wear 268 (2010) 294–301.

[9] V. Bushlya, F. Lenrick, J.-E. Ståhl, R. M'Saoubi, Influence of oxygen on the tool wear in machining, CIRP Annals 67 (1) (2018) 79–82.

[10] S.A. Klimenko, Y.A. Mukovoz, V.A. Lyashko, A.N. Vashchenko, V.V. Ogorodnik, On the wear mechanisms of cubic boron nitride base cutting tool, Wear 157 (1992)1–7.

[11] V.P. Bondarenko, A.P. Khalepa, E.S. Cherepanina, E.A. Pugach, Chemical interaction of cubic boron nitride with nickel, Synthetic Diamonds 6 (1978) 15–18 (in Russian).

[12] K. Shintani, H. Kato, T. Maeda, Y. Fujimura, A. Yamamoto, Cutting performance of CBN tools in machining of nickel based superalloy, Journal of Japan Society for Precision Engineering 58 (10) (1992) 1685-1690.

[13] Stahl J.-E., Metals Cutting: Theories and Models, SECO TOOLS, Fagersta, Sweden (2012).

[14] V.M. Bushlya, O.A. Gutnichenko, J.M. Zhou, J.-E. Ståhl, S. Gunnarsson, Tool wear and tool life of PCBN, binderless cBN and wBN-cBN tools in continuous finish hard turning of cold work tool steel, Journal of Superhard Materials 36 (1) (2014) 49–60.

[15] R. M'Saoubi, T. Larsson, J. Outeiro, Y. Guo, S. Suslov, C. Saldana, S. Chandrasekar, Surface integrity analysis of machined Inconel 718 over multiple length scales, CIRP Annals Manufacturing Technology 61 (2012) 99–102.

[16] Zhe Chen, Magnus Hörnqvist Colliander, Gustav Sundell, Ru Lin Peng, Jinming Zhou, Sten Johansson, Johan Moverare, Nano-scale characterization of white layer in broached Inconel 718, Materials Science and Engineering A 684 (2017) 373–384.

[17] Y. Le Godec, G. Hamel, D. Martinez-Garcia, T. Hammouda, V.L. Solozhenko, S. Klotz, Compact multianvil device for in situ studies at high pressures and temperatures, High-Press. Res. 25 (2005)243–253.

[18] V.L. Solozhenko, G. Will, F. Elf, Isothermal compression of hexagonal graphite-like boron nitride up to 12 GPa, Solid State Communications, 96 (1) (1995) 1–3.

[19] L.G. Khvostantsev, L.F. Vereschagin. A.P. Novikov, Device of toroid type for high pressure generation, High Temp.-High Press 9 (1977) 637–639.

[20] J. O. Andersson, T. Helander, L. Höglund. Thermo-Calc & DICTRA, Computational Tools for Materials Science, Calphad, 26 (2002).

[21] S.H. Fu, J.X. Dong, M.C. Zhang, X.S. Xie, Alloy design and development of INCONEL718 type alloy, Materials Science and Engineering A 499 (1–2) (2009) 215–220.

[22] Springer Materials' database: https://materials.springer.com/ (last accessed 2018-12-10).

[23] K. Frisk, A revised thermodynamic description of the Ti-C system, Computer Coupling of Phase Diagrams and Thermochemistry 27 (2003) 367–373.

[24] F. Liu, J. Xu, D. Zhang, Z. Jian, Solidification of highly undercooled hypereutectic Ni-Ni3B alloy melt, Metallurgical and Materials Transactions A: Physical Metallurgy and Materials Science, 45 (11) (2014) 4810–4819.